The Astrophysical Journal, 799:122 (7pp), 2015 February 1 doi:10.1088/0004-637X/799/2/122

NUSTAR AND *XMM-NEWTON* OBSERVATIONS OF THE EXTREME ULTRALUMINOUS X-RAY SOURCE NGC 5907 ULX1: A VANISHING ACT

D. J. Walton[1,2], F. A. Harrison[2], M. Bachetti[3,4], D. Barret[3,4], S. E. Boggs[5], F. E. Christensen[6], W. W. Craig[5], F. Fuerst[2], B. W. Grefenstette[2], C. J. Hailey[7], K. K. Madsen[2], M. J. Middleton[8], V. Rana[2], T. P. Roberts[9], D. Stern[1], A. D. Sutton[9], N. Webb[3,4], and W. Zhang[10]

[1] Jet Propulsion Laboratory, California Institute of Technology, Pasadena, CA 91109, USA
[2] Space Radiation Laboratory, California Institute of Technology, Pasadena, CA 91125, USA
[3] Universite de Toulouse, UPS-OMP, IRAP, Toulouse, France
[4] CNRS, IRAP, 9 Av. colonel Roche, BP 44346, F-31028 Toulouse cedex 4, France
[5] Space Sciences Laboratory, University of California, Berkeley, CA 94720, USA
[6] DTU Space, National Space Institute, Technical University of Denmark, Elektrovej 327, DK-2800 Lyngby, Denmark
[7] Columbia Astrophysics Laboratory, Columbia University, New York, NY 10027, USA
[8] Institute of Astronomy, University of Cambridge, Madingley Road, Cambridge CB3 0HA, UK
[9] Department of Physics, Durham University, South Road, Durham DH1 3LE, UK
[10] NASA Goddard Space Flight Center, Greenbelt, MD 20771, USA
Received 2014 August 19; accepted 2014 November 21; published 2015 January 21

ABSTRACT

We present results obtained from two broadband X-ray observations of the extreme ultraluminous X-ray source (ULX) NGC 5907 ULX1, known to have a peak X-ray luminosity of $\sim 5 \times 10^{40}$ erg s^{-1}. These *XMM-Newton* and *NuSTAR* observations, separated by only $\sim$4 days, revealed an extreme level of short-term flux variability. In the first epoch, NGC 5907 ULX1 was undetected by *NuSTAR*, and only weakly detected (if at all) with *XMM-Newton*, while in the second NGC 5907 ULX1 was clearly detected at high luminosity by both missions. This implies an increase in flux of $\sim$2 orders of magnitude or more during this $\sim$4 day window. We argue that this is likely due to a rapid rise in the mass accretion rate, rather than to a transition from an extremely obscured to an unobscured state. During the second epoch we observed the broadband 0.3–20.0 keV X-ray luminosity to be $(1.55 \pm 0.06) \times 10^{40}$ erg s^{-1}, similar to the majority of the archival X-ray observations. The broadband X-ray spectrum obtained from the second epoch is inconsistent with the low/hard accretion state observed in Galactic black hole binaries, but is well modeled with a simple accretion disk model incorporating the effects of photon advection. This strongly suggests that when bright, NGC 5907 ULX1 is a high-Eddington accretor.

Key words: black hole physics – X-rays: binaries – X-rays: individual (NGC 5907 ULX1)

1. INTRODUCTION

Ultraluminous X-ray sources (ULXs) are off-nuclear point sources with X-ray luminosities that exceed the Eddington limit for the $\sim 10\,M_{\odot}$ "stellar-mass" black holes observed in Galactic black hole binaries (BHBs; e.g., Orosz 2003), i.e., $L_{\rm X} > 10^{39}$ erg s^{-1}. Multi-wavelength observations have largely excluded highly anisotropic emission that could artificially increase the estimated luminosity (e.g., Berghea et al. 2010; Moon et al. 2011). The observed luminosities therefore require either the presence of larger black holes than those observed in our own galaxy (e.g., Miller et al. 2004; Strohmayer & Mushotzky 2009; Zampieri & Roberts 2009), or super-Eddington modes of accretion (e.g., Poutanen et al. 2007; Finke & Böttcher 2007). For recent reviews focusing on ULXs, see Roberts (2007) and Feng & Soria (2011).

Although the majority of ULXs only have luminosities marginally in excess of 10^{39} erg s^{-1} (Walton et al. 2011b; Swartz et al. 2011), and therefore likely represent a high luminosity extension of the stellar mass BHB population (Middleton et al. 2013; Liu et al. 2013; Motch et al. 2014), a smaller population of extreme sources have observed X-ray luminosities of $L_{\rm X} > 10^{40}$ erg s^{-1} (e.g., Farrell et al. 2009; Walton et al. 2011a; Jonker et al. 2012). The extreme luminosities displayed by these sources are of substantial interest, and mean they remain among the best candidates to host black holes more massive than those observed in Galactic BHBs.

NGC 5907 ULX1 is a luminous member of this population of extreme ULXs. The source was initially reported in the ULX catalog presented in Walton et al. (2011b) with a peak X-ray luminosity of $\sim 5 \times 10^{40}$ erg s^{-1} (see also Sutton et al. 2012). Although X-ray data on the edge-on spiral galaxy NGC 5907 is relatively sparse, since the discovery of ULX1 a number of follow-up observations have been undertaken with *XMM-Newton*, *Chandra*, and *Swift*, revealing the source to be variable by a factor of a few, confirming that a single, accretion powered source dominates the observed X-ray flux (Sutton et al. 2013a). Based on data with a bandpass limited to $E < 10$ keV, the observed characteristics of NGC 5907 ULX1 below 10 keV appear to be broadly consistent with a BHB in the sub-Eddington low/hard state (Sutton et al. 2012; see Remillard & McClintock 2006 for details on the standard BHB accretion states), implying the possible presence of a very massive black hole. However, the highest quality soft X-ray data available tentatively suggest the presence of a spectral break above $\sim$5 keV (Sutton et al. 2013a), which, if confirmed, would be inconsistent with this accretion regime, and potentially identify NGC 5907 ULX1 as a high-Eddington source (Gladstone et al. 2009).

The *Nuclear Spectroscopy Telescope Array* (*NuSTAR*; Harrison et al. 2013), in conjunction with *XMM-Newton*, *Suzaku*, and *Chandra*, has been providing the first ever high quality broadband X-ray spectra for a sample of known ULXs (see Bachetti et al. 2013, 2014; Rana et al. 2014; Walton et al. 2013a, 2014). Here we present results from the recent

Table 1
Details of the X-Ray Observations of NGC 5907 ULX1 Considered in This Work

Mission	OBSID	Start Date	Good Exposure[a] (ks)
	Epoch 1		
NuSTAR	30002039002	2013 Nov 6	45
NuSTAR	30002039003	2013 Nov 6	69
XMM-Newton	0724810201	2013 Nov 6	22/26
	Epoch 2		
NuSTAR	30002039005	2013 Nov 12	113
XMM-Newton	0724810401	2013 Nov 12	24/34
	Archival		
Chandra	12987	2012 Feb 11	11
Chandra	14391	2012 Feb 11	12
Swift	00032764001	2013 Mar 19	4
Swift	00032764002	2013 Apr 3	4
Swift	00032764003	2013 Apr 4	4
Swift	00032764004	2013 Apr 6	3.5
Swift	00032764005	2013 Apr 10	3.5
Swift	00032764006	2013 May 4	4

Note. [a] *XMM-Newton* exposures are listed for the EPIC-pn/MOS detectors.

NuSTAR and *XMM-Newton* observations of NGC 5907 ULX1. The paper is structured as follows: Section 2 describes our observations and data reduction procedure, and Sections 3, 4, and 5 describe the analysis performed. Finally, we discuss our results and conclusions in Section 6.

2. OBSERVATIONS AND DATA REDUCTION

During 2013 the *NuSTAR* and *XMM-Newton* X-ray observatories performed two coordinated observations of NGC 5907 ULX1, with some portion of the *NuSTAR* observation simultaneous with *XMM-Newton* in both cases (see Table 1 for details). Here, we outline our general data reduction procedure for these observations; details specific to each epoch are given in Sections 3 and 4.

2.1. NuSTAR

NuSTAR performed two observations of NGC 5907 ULX1 in late 2013, referred to throughout this work as epochs 1 and 2 (see Table 1; although the first epoch is comprised of two OBSIDs, it is actually one continuous observation). The start of the second observation is roughly a week after the start of the first, however given the duration, the period between the end of the first observation and the start of the second is only ∼4 days. We reduced the *NuSTAR* data using the standard pipeline (NUPIPELINE), part of the *NuSTAR* Data Analysis Software v1.3.1 (NUSTARDAS; included in the HEASOFT distribution as of version 6.14), and we use instrumental calibration files from *NuSTAR* caldb v20131223 throughout. The unfiltered event files were cleaned with the standard depth correction, significantly reducing the internal background at high energies, and passages through the South Atlantic Anomaly were removed. Source and background products were extracted from the cleaned event files for both focal plane modules (FPMA and FPMB) using NUPRODUCTS, with the background primarily estimated from a blank area of the same detector in each case (unless stated otherwise).

2.2. XMM-Newton

Each of the two *NuSTAR* observations was coordinated with a shorter observation with *XMM-Newton*, providing soft X-ray coverage down to ∼0.3 keV. Data reduction was carried out with the *XMM-Newton* Science Analysis System (SAS v13.5.0) in accordance with the standard prescription provided in the online guide.[11] The raw observation data files were processed using EPCHAIN and EMCHAIN to produce cleaned event lists for the EPIC-pn (Strüder et al. 2001) and EPIC-MOS (Turner et al. 2001) detectors, respectively. In this work, we use only single and double events (single to quadruple events) for EPIC-pn (EPIC-MOS), and exclude periods of high background flares (adopting thresholds of 0.5 and 0.12 ct s^{-1} in the 10–12 keV light curve from the full field of view for EPIC-pn and each EPIC-MOS detector, respectively). Science products were extracted using XMMSELECT, with the background estimated from areas of the same CCD free of contaminating point sources. Redistribution matrices and auxiliary response files were generated with RMFGEN and ARFGEN. After performing the data reduction separately for each of the two EPIC-MOS detectors, and confirming their consistency, these spectra were combined using the FTOOL ADDASCASPEC.

Throughout this work we perform spectral analysis with XSPEC v12.8.1 (Arnaud 1996), and all models include neutral absorption from both the Galactic column ($N_{\rm H;Gal} = 1.21 \times 10^{20}$ $\rm cm^{-2}$ toward NGC 5907; Kalberla et al. 2005), and an intrinsic absorption column at the redshift of NGC 5907 ($z = 0.002225$)[12] which is free to vary. Neutral absorption is treated with TBNEW,[13] the latest version of the TBABS absorption code (Wilms et al. 2000), with the appropriate solar abundances. Uncertainties are quoted at the 90% confidence level for one parameter of interest, unless stated otherwise. Where possible, the *XMM-Newton* and *NuSTAR* data are modeled simultaneously with all physical parameters linked between the different data sets; the spectral agreement between *XMM-Newton* and *NuSTAR* in their common 3–10 keV bandpass is known to be fairly good (Walton et al. 2013a, 2014), and we account for residual flux cross-calibration uncertainties between the EPIC-pn and EPIC-MOS detectors (*XMM-Newton*) and FPMA and FPMB (*NuSTAR*) by allowing multiplicative constants to float between them (fixing EPIC-pn to unity).

3. EPOCH 1

Based on the previously published observations, the X-ray emission from NGC 5907 ULX1 appears to be fairly persistent (Sutton et al. 2013a). However, during the first epoch reported here, no single point source obviously dominates the emission at the position of the ULX (Figure 1, left panel). Instead, the soft X-ray emission observed by *XMM-Newton* from the immediate vicinity of the ULX appears to be comprised of a series of faint sources (Figure 1, right panel), which even in combination do not result in a detection with *NuSTAR*. One of these sources is close to the known position of the ULX, and we therefore extract the *XMM-Newton* spectrum of this source from a circular region of radius 12″ to avoid contamination from the other sources. Fewer than 50 net source counts are detected in total (EPIC-pn+EPIC-MOS) in the 0.3–10.0 keV bandpass, so we rebin the data from this epoch to have a minimum of five counts per bin (before background subtraction) to maintain spectral

[11] http://xmm.esac.esa.int/
[12] From the NASA Extragalactic Database: http://ned.ipac.caltech.edu/
[13] http://pulsar.sternwarte.uni-erlangen.de/wilms/research/tbabs

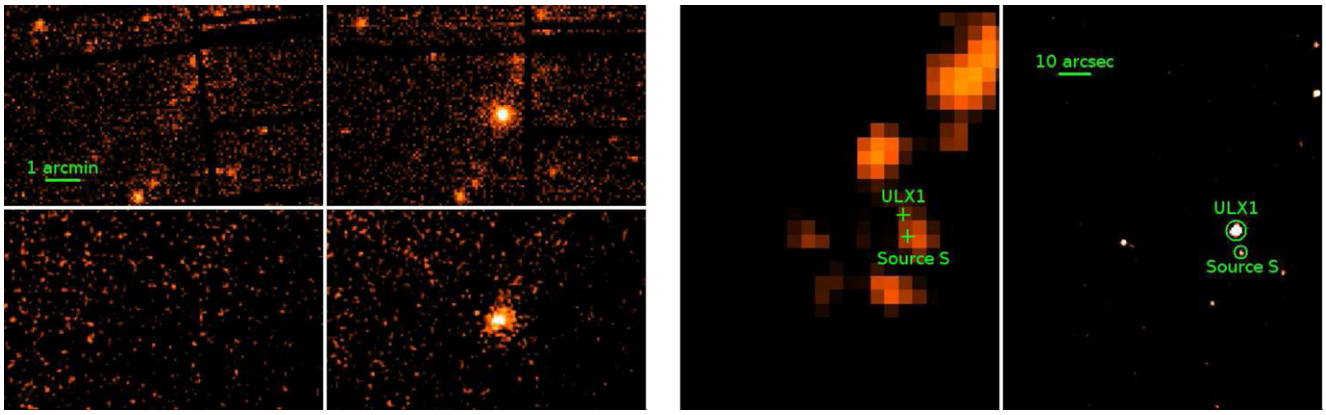

Figure 1. Left figure: four-panel image from the *XMM-Newton* (EPIC-pn, top panels) and *NuSTAR* (FPMA; bottom panels) observations of NGC 5907 ULX1 from the first (left panels) and second epochs (right panels). The ULX is clearly detected in the second epoch, but is either very weak or absent in the first. Right figure: zoom in on the immediate vicinity around the position of the ULX in the *XMM-Newton* image from the first epoch (left panel), and the same region from archival *Chandra* data (right panel); these images have been additionally smoothed for clarity. A number of faint sources are seen in the *XMM-Newton* data during this epoch, including one close to the position of the ULX. However, this is likely to be dominated by the faint source seen to the south of the ULX in the *Chandra* image (Source S; see Section 5.1).

coverage, and minimize the Cash statistic (Cash 1979) when analyzing these data. Here, the background contributes ∼45% of the total counts from the source region.

With so few counts it is not possible to undertake detailed spectral modeling, but to estimate a source flux we model the spectrum with a simple absorbed powerlaw, assuming $\Gamma = 1.7$ based on previous *XMM-Newton* observations (Sutton et al. 2012). We find an observed 0.3–10.0 keV flux of $F_{\rm Epoch1} = 11^{+5}_{-3} \times 10^{-15}$ erg cm^{-2} s^{-1} (throughout this work fluxes are estimated with CFLUX), substantially lower than any flux observed from NGC 5907 ULX1 to date (Sutton et al. 2013a). For a distance to NGC 5907 of 13.4 Mpc (Tully et al. 2009), the corresponding 0.3–10.0 keV luminosity is $2.4^{+1.1}_{-0.7} \times 10^{38}$ erg s^{-1}.

4. EPOCH 2

We find that NGC 5907 ULX1 is very clearly detected by both *XMM-Newton* and *NuSTAR* in the second epoch (see Figure 1), suggesting a remarkable flux transition in a fairly short space of time (the end of the first *NuSTAR* observation and the start of the second are separated by ∼4 days). We extracted spectra using a circular region of radius 21″ for *XMM-Newton*, chosen to simultaneously maximize the signal-to-noise for the ULX and minimize the contamination from the fainter sources nearby, and of radius 50″ for *NuSTAR*, given its larger point-spread function (PSF). In order to improve the statistics at the highest energies, we combine the spectra obtained by FPMA and FPMB with ADDASCASPEC (after confirming their consistency), and rebin all the spectra from this epoch to a minimum of 25 counts per bin, minimizing χ^2 in our analysis of these data. We obtain a detection in *NuSTAR* up to just over 20 keV.

Figure 2 shows the broadband 0.3–25.0 keV spectrum obtained from epoch 2. The *NuSTAR* data confirm the presence of a spectral break in the ∼3–10 keV bandpass, similar to other ULXs observed by *NuSTAR* to date (Bachetti et al. 2013; Rana et al. 2014; Walton et al. 2013a, 2014). As the data for NGC 5907 ULX1 from this epoch are of much lower quality compared to the broadband observations of those other ULX targets, we limit our spectral analysis in this work to simple continuum modeling of the time averaged spectrum; the count rates obtained unfortunately do not permit detailed variability studies of these data (0.12 and 0.04 ct s^{-1} in 0.3–10.0 keV from EPIC-pn and each EPIC-MOS detector, and 0.008 ct s^{-1} in 3–25 keV from each *NuSTAR* FPM). Both Galactic and intrinsic neutral absorption are included in all models. In addition, given the larger extraction region used for the *NuSTAR* data, we also investigate whether the results presented below are influenced by undetected contamination from the other sources seen in the epoch 1 *XMM-Newton* data (Figure 1), and we repeat our analysis using the epoch 1 *NuSTAR* spectrum extracted from the epoch 2 source region as an alternative background spectrum. We obtain consistent results with both background estimations, and we therefore only present those obtained with the epoch 2 background for simplicity.

Table 2
Best-fit Parameters Obtained for the Simple Continuum Models Applied to the Broadband Spectrum Observed from NGC 5907 ULX1 During Epoch 2

Model	POWERLAW	DISKBB	DISKPBB
$N_{\rm H}$ (10^{21} cm^{-2})	9.3 ± 0.6	3.4 ± 0.3	6.7 ± 0.7
Γ	2.14 ± 0.06	...	...
$T_{\rm in}$ (keV)	...	1.90 ± 0.07	2.9 ± 0.3
p	...	...	0.55 ± 0.02
χ^2/DoF	403/277	393/277	286/276

We first fit the broadband spectrum with an absorbed powerlaw model, but find that this provides a poor fit ($\chi^2_\nu = \chi^2/{\rm DoF} = 403/277$; see Table 2), and results in systematic residuals across the whole bandpass (see Figure 2, right panel). In particular, the model overpredicts the highest energies, confirming the existence of spectral curvature above ∼3 keV. We also find that a model consisting of a geometrically thin, optically thick accretion disk (DISKBB; Mitsuda et al. 1984; see also Shakura & Sunyaev 1973) provides a poor fit ($\chi^2_\nu = 393/277$), clearly underestimating the high energy flux. However, a slightly more complex accretion disk model in which the radial temperature index (p) is free to vary (DISKPBB; Mineshige et al. 1994) does provides a good fit across the full bandpass ($\chi^2_\nu = 286/276$), and there is no obvious requirement for any additional spectral components. The radial temperature index of $p = 0.55 \pm 0.02$ obtained (see Table 2) is shallower than expected for a thin accretion disk ($p_{\rm thin} = 0.75$), consistent with an accretion disk in which strong advection of radiation occurs, as may be expected at very high accretion rates where radiation pressure should dominate and modify the disk structure (e.g., Abramowicz et al. 1988).

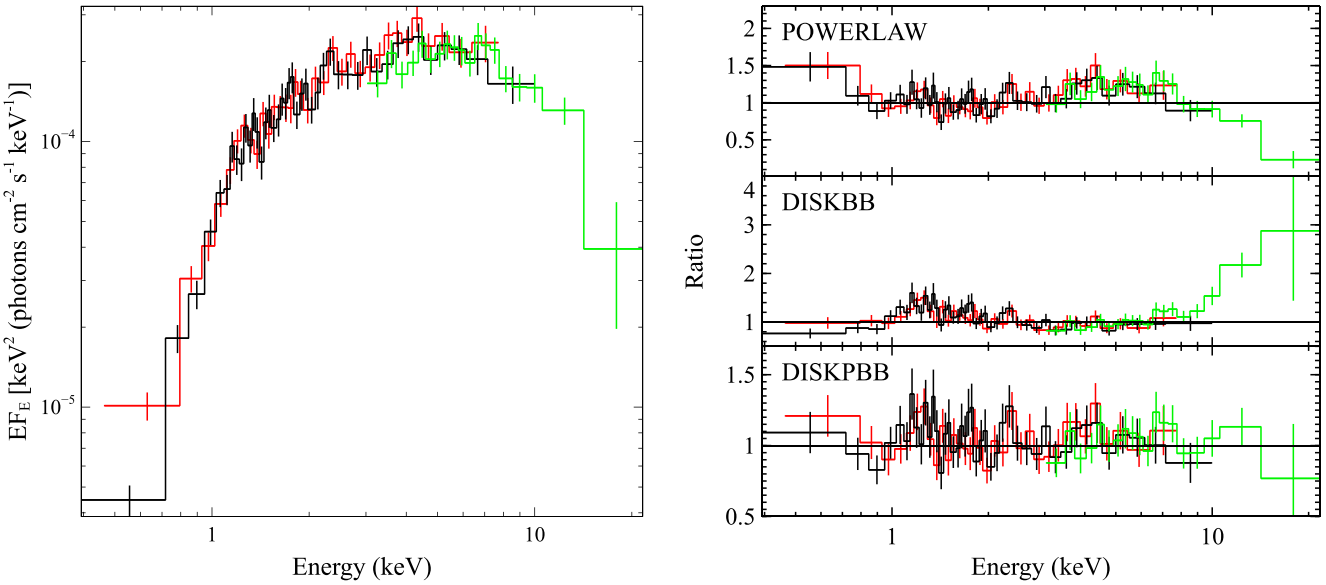

Figure 2. Left panel: the broadband *XMM-Newton*+*NuSTAR* X-ray spectrum of NGC 5907 ULX1 obtained from epoch 2. The data have been unfolded through a model, which is simply constant with energy. The *XMM-Newton* EPIC-pn and EPIC-MOS data are shown in black and red, respectively, and the *NuSTAR* FPM data are shown in green. Right panels: data/model ratios for the continuum models applied to the epoch 2 spectrum (see Section 4). In all panels, the data have been rebinned for visual clarity.

Table 3
Observed Fluxes from the Data Sets Analyzed in This Work

Data Set	0.3–10.0 keV Flux	0.3–20.0 keV Flux
	(10^{-15} erg cm^{-2} s^{-1})	
Epoch 1[a]	11^{+5}_{-3}	...
Epoch 2	630^{+30}_{-20}	720 ± 30
2013 *Swift*	30^{+20}_{-10}	...
Source S (*Chandra*)	7 ± 3	...

Notes. The *Chandra* flux for Source S is also listed for comparison.
[a] Likely dominated by emission from Source S, see Section 5.1.

Based on the DISKPBB model we find an observed 0.3–20.0 keV X-ray flux for NGC 5907 ULX1 during the second epoch of $F_{\rm Epoch2} = (7.2 \pm 0.3) \times 10^{-13}$ erg cm^{-2} s^{-1}, ~87% of which falls in the 0.3–10.0 keV bandpass. The observed fluxes of the various data sets considered in this work are summarized in Table 3. This equates to a broadband X-ray luminosity of $(1.55 \pm 0.06) \times 10^{40}$ erg s^{-1} even before any absorption correction. While extreme for the ULX population, this is still a factor of ~2–3 lower than the peak luminosity of ~5 $\times 10^{40}$ erg s^{-1} (0.3–10.0 keV) that has been observed from this source (Sutton et al. 2013a).

5. ARCHIVAL DATA

5.1. Chandra Imaging and Astrometry

To determine the ULX flux during epoch 1 it is essential to address the level of source confusion. We inspected the archival data obtained with the *Chandra* observatory (Weisskopf et al. 2002; see Table 1), which reveal a faint source ~6–7″ to the south of NGC 5907 ULX1 (hereafter Source S; see Figure 1). In order to assess whether the *XMM-Newton* detection could be associated with Source S, rather than with the ULX, we extracted the *Chandra* spectrum of Source S. Both *Chandra* observations were taken in the Timed Event mode, and we extracted spectra from the ACIS-S detector (Garmire et al. 2003) using the standard pipeline in CIAO v4.6. The source spectrum was obtained from a circular region of radius ~2″, while the background was extracted from a larger circular region of radius ~13″ that was free from any other contaminating sources. The ACIS spectra from the two observations were combined using ADDASCASPEC. Very few net source counts are detected (fewer than 15), so we rebin the spectrum to a minimum of two counts per bin and again minimize the Cash statistic when considering these data. In this case, the background contributes only ~10% of the total counts from the source region. Applying the same model used for the detection from epoch 1 to the *Chandra* data for Source S, we find an observed 0.3–10.0 keV flux of $F_{\rm SourceS} = (7 \pm 3) \times 10^{-15}$ erg cm^{-2} s^{-1}. This is consistent with that obtained for the epoch 1 *XMM-Newton* observation (Section 3), which may suggest a common origin. Were this to be the case, the variability displayed by NGC 5907 ULX1 between epochs 1 and 2 would be even greater than implied by the measured *XMM-Newton* fluxes (Sections 3 and 4).

Unfortunately we were not able to reliably correct the *XMM-Newton* astrometry in epoch 1 against *Chandra* directly, owing to a lack of sources within the overlapping *XMM-Newton* and *Chandra* sky coverage. However, there are just about sufficient sources in the *XMM-Newton* field of view to determine whether there is any astrometric offset between epochs 1 and 2. To this end, we generated source lists for the EPIC-pn detector from both epochs using EDETECT_CHAIN, and then computed the astrometric correction between the two epochs using EPOSCORR (both part of the *XMM-Newton* SAS). This found five robust source matches (note that the ULX itself was excluded from the matching procedure). The best solution to the source matching found the offset between epochs to be $(2.7 \pm 0.1)''$ in Right Ascension and $(1.9 \pm 0.1)''$ in Declination, with no rotation component, such that epoch 2 is shifted to the South and the West relative to epoch 1. We used these offsets to correct the position obtained for ULX1 with EDETECT_CHAIN in epoch 2, when ULX1 dominated

the observed emission, to the coordinate system registered to the image from epoch 1. Having done so, we then also worked out the position of Source S in this image, using the relative positions of ULX1 and Source S determined from the *Chandra* data. These corrected positions are shown in the *XMM-Newton* image of epoch 1 in Figure 1. The peak of the faint emission from epoch 1 is more consistent with the position of Source S, although there may additionally be some even fainter extent to the emission toward the position of the ULX. Therefore, while there may still be some contribution from ULX1, we conclude that the emission detected in epoch 1 is likely dominated by Source S.

5.2. 2013 Swift Snapshots

A series of six short observations were undertaken in 2013 by *Swift* (Gehrels et al. 2004) prior to our broadband observations (between March and May, see Table 1 for details), which were not included in Sutton et al. (2013a). We inspected these data in order to provide further context for the extreme low flux observed in epoch 1. Although the earlier 1–2 ks *Swift* snapshots presented in Sutton et al. (2013a) easily detected NGC 5907 ULX1, it is not obviously detected by the XRT in any of the individual 2013 observations, despite their longer exposure (typically ∼4 ks), indicating a prolonged period at low flux earlier in 2013. However, although individual observations do not provide a clear detection, if we stack the 2013 observations, we do find a clear detection of a source at the position of NGC 5907 ULX1 in the combined data set.

We extracted the spectrum from this stacked data set, following the standard XRT reduction guide[14] in order to estimate the average source flux during this period. All the observations were obtained in the standard photon-counting mode, and we extracted the source spectrum from the same region used for the epoch 1 *XMM-Newton* data, estimating the background from a much larger region of radius 180″ avoiding the plane of NGC 5907 and other contaminating point sources. We used the latest XRT redistribution matrix available in the *Swift* CALDB, and generated the ancillary response file as standard for a point source on axis with XRTMKARF, correcting for PSF losses to account for the small extraction region. Very few net source counts are detected (∼10), so we rebin to a minimum of two counts per bin, and minimize the Cash statistic when analyzing these data. Here the background contribution is again very small, only ∼10% of the total counts from the source region.

Applying the same model used for the *XMM-Newton* detection from epoch 1, we find an average 0.3–10.0 keV flux of $F_{\rm Swift} = 30^{+20}_{-10} \times 10^{-15}$ erg cm^{-2} s^{-1} during the 2013 observations, implying a luminosity of $6^{+4}_{-3} \times 10^{38}$ erg s^{-1}. The *Swift* detection is a factor of ∼3 brighter than both the epoch 1 *XMM-Newton* detection, and Source S during the *Chandra* observations (albeit with admittedly large uncertainties). Although we obviously cannot exclude the possibility that Source S is also variable, given the extreme level of variability NGC 5907 ULX1 is now known to exhibit it seems natural to assume the variability between the 2013 *Swift* data and epoch 1 is also driven by NGC 5907 ULX1. This would suggest the *Swift* data constitute a detection of NGC 5907 ULX1, even if the epoch 1 *XMM-Newton* data potentially do not.

6. DISCUSSION AND CONCLUSIONS

We have presented an analysis of two epochs of broadband X-ray observations of the extreme ULX NGC 5907 ULX1 undertaken with *NuSTAR* and *XMM-Newton*. These observations reveal an astonishing level of X-ray flux variability between the two epochs. Although the source is not detected by *NuSTAR* in the first epoch, a clear detection is obtained in the second, providing the first constraints on the hard X-ray ($E > 10$ keV) emission. Broadly similar to the results obtained for other ULXs observed by *NuSTAR* to date (Bachetti et al. 2013; Rana et al. 2014; Walton et al. 2013a, 2014; E. S. Mukherjee et al., in preparation), we find the hard X-ray emission from NGC 5907 ULX1 to be very weak relative to that at lower energies (see Figure 2). During this epoch the broadband spectrum is not consistent with a $\sim 10^{3-4}$ $M_{\odot}$ intermediate mass black hole accreting in the low/hard state displayed by Galactic BHBs. Instead, the spectrum is well modeled with an advection dominated accretion disk (e.g., Abramowicz et al. 1988), confirming the spectral cutoff tentatively suggested by the archival *XMM-Newton* data (Sutton et al. 2013a), and implying that NGC 5907 ULX1 may be accreting at a very high, possibly super-Eddington rate.

The most intriguing aspect of these observations is the extreme level of flux variability. We show in Figure 3 a long-term X-ray light curve for NGC 5907 ULX1, adapted from Sutton et al. (2013a) to include our *XMM-Newton* and *NuSTAR* observations (and also the additional 2013 *Swift* data). Even assuming the faint source detected by *XMM-Newton* in epoch 1 is NGC 5907 ULX1, its observed flux varied by ∼2 orders of magnitude in ∼4 days (the flux appears stable throughout epoch 2, see the inset in Figure 3). However, given the flux observed by *Chandra* and the astrometric offset between the epoch 1 and epoch 2 *XMM-Newton* observations, the emission detected in epoch 1 is likely dominated by Source S (see Section 5.1), implying an even more extreme variation from ULX1. While there are transient ULXs that show orders of magnitude of variation (similar to low mass X-ray binaries, e.g., Middleton et al. 2013), even at peak luminosity these tend to be the fainter members of the ULX population. The brighter ULXs tend to be variable only by a factor of ∼a few, broadly similar to high mass X-ray binaries, (e.g., Kaaret et al. 2009; Kaaret & Feng 2009; Kong et al. 2010; Walton et al. 2013a). Until this work, the behavior observed from NGC 5907 ULX1 was similar to this latter population, consistent with its extreme luminosity.

Given the relatively persistent behavior observed previously one tantalizing possibility for the extreme low state observed in epoch 1 is that it may represent an eclipse of the X-ray source, perhaps by a stellar companion or by a warped outer accretion disk. If this were the case, the lack of a hard X-ray detection with *NuSTAR* suggests the medium eclipsing NGC 5907 ULX1 is extremely thick ($N_{\rm H} \sim 10^{24}$ cm^{-2} or more). However, the duration of the *NuSTAR* observation is ∼2 days (the low-earth orbit results in a ∼50% observing efficiency; Harrison et al. 2013), and we do not know how long this low flux persisted before the *NuSTAR* observation, thus if this were an eclipse by the companion star the orbital period would have to be $\gg$2 days. For comparison, the orbital period of the eclipsing black hole binary IC 10 X-1, the most massive dynamically constrained stellar remnant measured to date, is ∼34 hr (Prestwich et al. 2007; Silverman & Filippenko 2008), and the X-ray eclipses last ∼30% of this period, significantly shorter than the *NuSTAR* observation. The other eclipsing BHB system known, M 33 X-7, has an orbital period of ∼3.5 days, with the X-ray eclipses lasting ∼15% of this (Pietsch et al. 2006; Orosz et al. 2007). Nevertheless, GRS 1915+105, one of the Galactic sources widely considered most analogous to ULXs, has a much longer orbital period (∼34 days; Steeghs et al. 2013), and several

[14] http://swift.gsfc.nasa.gov/analysis/xrt_swguide_v1_2.pdf

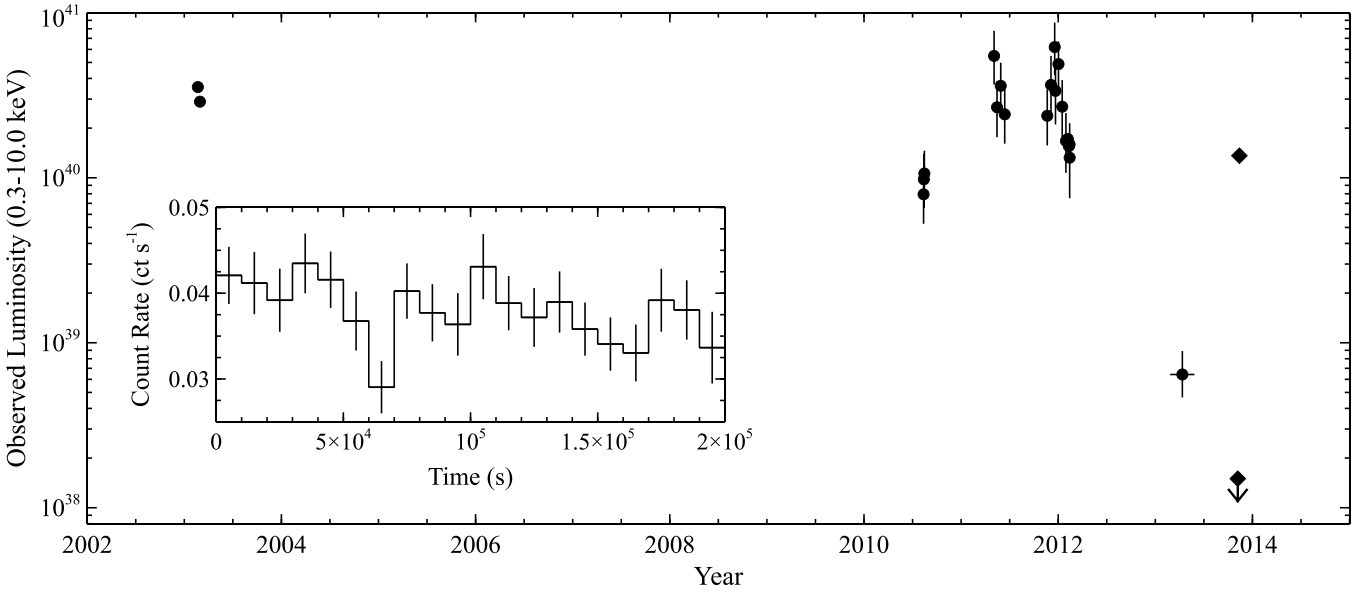

Figure 3. Long-term light curve observed from NGC 5907 ULX1 since its discovery by *XMM-Newton* in 2003 (adapted from Sutton et al. 2013a). Our most recent *XMM-Newton* and *NuSTAR* observations are indicated with diamonds, while archival observations with *XMM-Newton*, *Chandra*, and *Swift* are indicated with circles (see Sutton et al. 2013a for details). For consistency with Sutton et al. (2013a), we show 1σ errors here. Given that the detected emission from epoch 1 is dominated by Source S, we adopt a conservative upper limit on the flux from ULX1 during this epoch of half of the upper bound on the total flux observed by *XMM-Newton*, but we assume the combined 2013 *Swift* data does represent a detection of NGC 5907 ULX1. Inset: the *NuSTAR* (FPMA+FPMB) light curve observed from NGC 5907 ULX1 during epoch 2 (10 ks bins), displaying a relatively stable flux throughout the observation.

works have suggested that ULXs might plausibly have very long orbital periods (up to ∼100 days or more; Podsiadlowski et al. 2003; Pooley & Rappaport 2005; Madhusudhan et al. 2008) if they accrete from evolved stellar companions via Roche-lobe overflow, as suggested by the lack of iron emission (Walton et al. 2012, 2013b). If the eclipse is by some other material, e.g., the outer regions of a warped accretion disk rather than the stellar companion, this may precess on long, super-orbital timescales, and would ease the requirement for a long orbit. A scenario along these lines was proposed as a potential explanation for the rare (and generally less extreme) dips observed from the well studied, soft-spectrum ULX NGC 5408 X-1 (lasting up to a few days; Grisé et al. 2013). This behavior is perhaps analogous to the "dipping" low-mass X-ray binaries (e.g., Díaz Trigo et al. 2009).

The *Swift* observations earlier in 2013 represent an additional period of low flux that appears to last ∼6 weeks (although we note the infrequent observing cadence during this period). However, the flux during epoch 1 is fainter than that from the combination of these *Swift* observations though, and likely substantially so given that the epoch 1 emission is dominated by Source S. It may therefore be possible that we are observing the effect of an eclipse imprinted on top of a strong level of intrinsic variability. While it may not be possible to conclusively rule out an explanation along these lines with the current data, we do not consider this scenario to be particularly likely. Nevertheless, it is interesting to note that if this were the case, it would imply that we are viewing NGC 5907 ULX1 at a high inclination. This is at odds with the suggested framework of the wind dominated "ultraluminous state" for super-Eddington accretion in which hard spectrum ULXs similar to NGC 5907 ULX1 are viewed close to face on, such that the hot inner regions of the accretion flow are visible. For edge-on sources, the inner regions would instead be obscured by cooler material in a large scale-height wind launched from the disk, resulting in a soft X-ray spectrum (Sutton et al. 2013b; Middleton et al. 2014), inconsistent with that observed. If the variability does result from a high inclination, this would thus favor the "patchy disk" scenario suggested by Miller et al. (2014).

If the extreme rise in flux is not related to the end of an obscuration event, it must instead be caused by a rapid increase in the mass accretion rate onto NGC 5907 ULX1. Such rapid increases in flux are occasionally seen in Galactic X-ray binaries, and appear in some instances to be related to increased accretion, rather than obscuration (e.g., XTE J1701-407: Degenaar et al. 2011; Pawar et al. 2013, 4U 1700-377: Smith et al. 2012). In the most extreme cases, super-fast X-ray transients can flare by orders of magnitude in an extremely short period of time (hours or days, e.g., Sidoli et al. 2009), although these are very short-lived flare events at much lower luminosities which differ markedly from the behavior of NGC 5907 ULX1.

One scenario that can result in rapid rises in accretion rate is for the system to have a highly eccentric orbit, with large accretion bursts triggered close to periastron, broadly similar to Be/X-ray binaries (e.g., Reig 2011; Casares et al. 2014). This scenario is currently the leading interpretation for the almost periodic outbursts exhibited by the most extreme ULX observed to date, ESO 243-49 HLX1 ($L_{\rm X,peak} \sim 10^{42}$ erg s^{-1}), which displays a repeated "fast-rise-exponential-decay" (FRED) outburst profile with similarly large and rapid flux increases to those seen in our observations of NGC 5907 ULX1 (e.g., Lasota et al. 2011; Webb et al. 2014, although see King & Lasota 2014). Given the poor sampling to date of the long-term behavior of NGC 5907 ULX1, it is possible that something similar could be occurring in this case, albeit at a lower absolute luminosity, and with the source rising into a potentially super-Eddington state (in contrast, HLX-1 seems to exhibit the standard evolution shown by sub-Eddington Galactic binaries during its outbursts; Servillat et al. 2011; Godet et al. 2012). Thus it may be possible for the extreme variability observed to be related to the orbit of the system, without being associated with an eclipse event. In light of these observations, extended monitoring of this remarkable

source is strongly recommended in order to test this exciting possibility.

The authors would like to thank the reviewer for positive and useful feedback, which helped improve the manuscript, as well as Diego Altamarino for useful discussions. M.B. and D.B. acknowledge financial support from the French Space Agency (CNES). This research has made use of data obtained with the *NuSTAR* mission, a project led by the California Institute of Technology (Caltech), managed by the Jet Propulsion Laboratory (JPL) and funded by NASA, and has utilized the *NuSTAR* Data Analysis Software (NUSTARDAS) jointly developed by the ASI Science Data Center (ASDC, Italy) and Caltech (USA). This research has also made use of data obtained with *XMM-Newton*, an ESA science mission with instruments and contributions directly funded by ESA Member States and NASA, and NASA's *Chandra* and *Swift* satellites.

Facilites: NuSTAR, XMM, Chandra, Swift

REFERENCES

Abramowicz, M. A., Czerny, B., Lasota, J. P., & Szuszkiewicz, E. 1988, ApJ, 332, 646
Arnaud, K. A. 1996, in ASP Conf. Ser. 101 Astronomical Data Analysis Software and Systems V, ed. G. H. Jacoby & J. Barnes (San Francisco, CA: ASP), 17
Bachetti, M., Harrison, F. A., Walton, D. J., et al. 2014, Natur, 514, 202
Bachetti, M., Rana, V., Walton, D. J., et al. 2013, ApJ, 778, 163
Berghea, C. T., Dudik, R. P., Weaver, K. A., & Kallman, T. R. 2010, ApJ, 708, 364
Casares, J., Negueruela, I., Ribó, M., et al. 2014, Natur, 505, 378
Cash, W. 1979, ApJ, 228, 939
Degenaar, N., Wijnands, R., Altamirano, D., et al. 2011, ATel, 3654, 1
Díaz Trigo, M., Parmar, A. N., Boirin, L., et al. 2009, A&A, 493, 145
Farrell, S. A., Webb, N. A., Barret, D., Godet, O., & Rodrigues, J. M. 2009, Natur, 460, 73
Feng, H., & Soria, R. 2011, NAR, 55, 166
Finke, J. D., & Böttcher, M. 2007, ApJ, 667, 395
Garmire, G. P., Bautz, M. W., Ford, P. G., Nousek, J. A., & Ricker, G. R., Jr. 2003, Proc. SPIE, 4851, 28
Gehrels, N., Chincarini, G., Giommi, P., et al. 2004, ApJ, 611, 1005
Gladstone, J. C., Roberts, T. P., & Done, C. 2009, MNRAS, 397, 1836
Godet, O., Plazolles, B., Kawaguchi, T., et al. 2012, ApJ, 752, 34
Grisé, F., Kaaret, P., Corbel, S., Cseh, D., & Feng, H. 2013, MNRAS, 433, 1023
Harrison, F. A., Craig, W. W., Christensen, F. E., et al. 2013, ApJ, 770, 103
Jonker, P. G., Heida, M., Torres, M. A. P., et al. 2012, ApJ, 758, 28
Kaaret, P., & Feng, H. 2009, ApJ, 702, 1679
Kaaret, P., Feng, H., & Gorski, M. 2009, ApJ, 692, 653
Kalberla, P. M. W., Burton, W. B., Hartmann, D., et al. 2005, A&A, 440, 775
King, A., & Lasota, J.-P. 2014, MNRAS, 444, L30
Kong, A. K. H., Yang, Y. J., Yen, T.-C., Feng, H., & Kaaret, P. 2010, ApJ, 722, 1816
Lasota, J.-P., Alexander, T., Dubus, G., et al. 2011, ApJ, 735, 89
Liu, J.-F., Bregman, J. N., Bai, Y., Justham, S., & Crowther, P. 2013, Natur, 503, 500
Madhusudhan, N., Rappaport, S., Podsiadlowski, P., & Nelson, L. 2008, ApJ, 688, 1235
Middleton, M. J., Heil, L., Pintore, F., Walton, D. J., & Roberts, T. P. 2014, MNRAS, in press (arXiv:1412.4532)
Middleton, M. J., Miller-Jones, J. C. A., Markoff, S., et al. 2013, Natur, 493, 187
Miller, J. M., Bachetti, M., Barret, D., et al. 2014, ApJL, 785, L7
Miller, J. M., Raymond, J., Fabian, A. C., et al. 2004, ApJ, 601, 450
Mineshige, S., Hirano, A., Kitamoto, S., Yamada, T. T., & Fukue, J. 1994, ApJ, 426, 308
Mitsuda, K., Inoue, H., Koyama, K., et al. 1984, PASJ, 36, 741
Moon, D.-S., Harrison, F. A., Cenko, S. B., & Shariff, J. A. 2011, ApJL, 731, L32
Motch, C., Pakull, M. W., Soria, R., Grisé, F., & Pietrzyński, G. 2014, Natur, 514, 198
Orosz, J. A. 2003, in IAU Symp. 212, A Massive Star Odyssey: From Main Sequence to Supernova, ed. K. van der Hucht, A. Herrero, & C. Esteban (Cambridge: Cambridge Univ. Press), 365
Orosz, J. A., McClintock, J. E., Narayan, R., et al. 2007, Natur, 449, 872
Pawar, D. D., Kalamkar, M., Altamirano, D., et al. 2013, MNRAS, 433, 2436
Pietsch, W., Haberl, F., Sasaki, M., et al. 2006, ApJ, 646, 420
Podsiadlowski, P., Rappaport, S., & Han, Z. 2003, MNRAS, 341, 385
Pooley, D., & Rappaport, S. 2005, ApJL, 634, L85
Poutanen, J., Lipunova, G., Fabrika, S., Butkevich, A. G., & Abolmasov, P. 2007, MNRAS, 377, 1187
Prestwich, A. H., Kilgard, R., Crowther, P. A., et al. 2007, ApJL, 669, L21
Rana, V., Harrison, F. A., Bachetti, M., et al. 2014, ApJ, in press (arXiv:1401.4637)
Reig, P. 2011, Ap&SS, 332, 1
Remillard, R. A., & McClintock, J. E. 2006, ARA&A, 44, 49
Roberts, T. P. 2007, Ap&SS, 311, 203
Servillat, M., Farrell, S. A., Lin, D., et al. 2011, ApJ, 743, 6
Shakura, N. I., & Sunyaev, R. A. 1973, A&A, 24, 337
Sidoli, L., Romano, P., Mangano, V., et al. 2009, ApJ, 690, 120
Silverman, J. M., & Filippenko, A. V. 2008, ApJL, 678, L17
Smith, D. M., Markwardt, C. B., Swank, J. H., & Negueruela, I. 2012, MNRAS, 422, 2661
Steeghs, D., McClintock, J. E., Parsons, S. G., et al. 2013, ApJ, 768, 185
Strohmayer, T. E., & Mushotzky, R. F. 2009, ApJ, 703, 1386
Strüder, L., Briel, U., Dennerl, K., et al. 2001, A&A, 365, L18
Sutton, A. D., Roberts, T. P., Gladstone, J. C., et al. 2013a, MNRAS, 434, 1702
Sutton, A. D., Roberts, T. P., & Middleton, M. J. 2013b, MNRAS, 435, 1758
Sutton, A. D., Roberts, T. P., Walton, D. J., Gladstone, J. C., & Scott, A. E. 2012, MNRAS, 423, 1154
Swartz, D. A., Soria, R., Tennant, A. F., & Yukita, M. 2011, ApJ, 741, 49
Tully, R. B., Rizzi, L., Shaya, E. J., et al. 2009, AJ, 138, 323
Turner, M. J. L., Abbey, A., Arnaud, M., et al. 2001, A&A, 365, L27
Walton, D. J., Fuerst, F., Harrison, F., et al. 2013a, ApJ, 779, 148
Walton, D. J., Gladstone, J. C., Roberts, T. P., et al. 2011a, MNRAS, 414, 1011
Walton, D. J., Harrison, F. A., Grefenstette, B. W., et al. 2014, arXiv:1402.2992
Walton, D. J., Miller, J. M., Harrison, F. A., et al. 2013b, ApJL, 773, L9
Walton, D. J., Miller, J. M., Reis, R. C., & Fabian, A. C. 2012, MNRAS, 426, 473
Walton, D. J., Roberts, T. P., Mateos, S., & Heard, V. 2011b, MNRAS, 416, 1844
Webb, N. A., Cseh, D., & Kirsten, F. 2014, PASA, 31, 9
Weisskopf, M. C., Brinkman, B., Canizares, C., et al. 2002, PASP, 114, 1
Wilms, J., Allen, A., & McCray, R. 2000, ApJ, 542, 914
Zampieri, L., & Roberts, T. P. 2009, MNRAS, 400, 677